Korean J. Chem. Eng., 40(8), 1986-1992 (2023)
DOI: 10.1007/s11814-023-1465-4

pISSN: 0256-1115
eISSN: 1975-7220

Effect of pyrolysis temperature on the physiochemical properties of biochars produced from raw and fermented rice husks

Sana Hafiza[*,,‡], Asim Riaz[***,‡], Zubaria Arshad[**], Syeda Tahsin Zahra[**], Javaid Akhtar[****], Sumaira Kanwal[*****], Hassan Zeb[**,†], and Jaehoon Kim[******,*******,********,†]**

*Zhengzhou University, Henan, China
**Institute of Energy and Environmental Engineering, University of the Punjab, Pakistan
***Department of Chemical Engineering, Khwaja Fareed University of Engineering & Information Technology, Rahim Yar Khan
****Institute of Chemical Engineering and Technology, University of the Punjab, Pakistan
*****Department of Environmental Sciences, University of Narowal
******SKKU Advanced Institute of Nanotechnology (SAINT), Sungkyunkwan University, 2066 Seobu-ro, Jangan-gu, Suwon, Gyeonggi-do 16419, Korea
*******School of Mechanical Engineering, Sungkyunkwan University, 2066 Seobu-ro Jangan-gu, Suwon, Gyeonggi-do 16419, Korea
********School of Chemical Engineering, Sungkyunkwan University, 2066 Seobu-ro, Jangan-gu, Suwon, Gyeonggi-do 16419, Korea
(*Received 18 December 2022 • Revised 14 March 2023 • Accepted 31 March 2023*)

Abstract−This study investigated the slow pyrolysis behavior of raw rice husk (RRH) and fermented rice husk (FRH) in a fixed-bed reactor at temperatures in the range of 200-600 °C. The effects of pyrolysis temperature on the biochar yield, composition, and physiochemical properties were examined to evaluate the energy potential of biochars produced from RRH and FRH. The FRH-derived biochar produced at 600 °C was found to be more suitable than the RRH-derived biochar because of its higher carbon content (68.9% vs 42.1%), GCV (31.6 vs 24.1 MJ kg^{-1}), and true density (1.94 vs 1.54 g cm^{-3}). The slow pyrolysis in the high-temperature regime facilitated the formation of lignin-rich and aromatically condensed biochar, making it particularly useful for producing carbon-rich materials. Thus, slow pyrolysis can be a technically viable approach for producing high-energy-density solid fuels that can replace medium-ranking coals in co-firing.

Keywords: Rice Husk, Fermented Residue, Slow Pyrolysis, Biochar, Physiochemical Characterization

INTRODUCTION

As an alternative to conventional sources of energy, such as fossil fuels, lignocellulosic biomass feedstock derived from agricultural, forest, and industrial wastes has been extensively studied as a potential renewable resource to produce biofuels, biochemicals, and carbon-based products [1,2]. Lignocellulosic biomass is mainly composed of cellulose, hemicellulose, and lignin. Conventionally, the complex structure of lignocellulosic biomass has been deconstructed to produce biofuels and biochemicals, by cleaving chemical bonds between the constituent polymers using energy-intensive pretreatment techniques [3]. The pretreatment improves the accessibility of intermediates for their subsequent chemical and biological conversions into final products [4]. Although practical-scale conversion technologies are still in their infancy, the vast availability, non-edibility, renewability, and carbon neutrality of lignocellulosic biomass are the main attributes that motivate researchers to develop efficient conversion strategies [5,6].

Pakistan is an agricultural country that harvests a large quantity of lignocellulosic biomass; for example, an average of 6 million tons of rice per year is produced in Pakistan, which is ranked as the world's 11th largest rice producer [7,8]. Rice grains are mechanically separated from paddy straw during harvesting, yielding rice husk as a natural byproduct. Rice husk accounts for approximately 20% of the paddy weight; because of the high rice production rate, 770 million tons of rice husk is generated annually in Asian countries. Rice husk is mainly composed of cellulose, lignin, and mineral ash [9]. Owing to its high organic content and wide availability, rice husk has a good potential as a renewable and sustainable feedstock in realizing practical-scale biorefineries. However, due to the lack of suitable conversion methods, rice husks are burnt to reduce their volume. This direct combustion of rice husk may potentially lead to the emission of fibrous and crystalline silica-based particulate matters (PMs) [10]. The combustion and disposal method can be a biohazard that is extremely harmful to the environment. In this context, developing an efficient thermochemical conversion method for rice husks is crucial not only to harness eco-friendly and energy-

†To whom correspondence should be addressed.
E-mail: hassanzeb.ieee@pu.edu.pk, jaehoonkim@skku.edu
‡Both the authors have contributed equally.

dense biofuels but also to solve disposal issues [5].

The gasification of rice husks can be an alternative to combustion, producing valuable syngas (mixture of CO and H_2). However, gasification technologies demand huge capital investments, significantly greater than those required by conventional fossil-fuel conversion techniques [11]. Pyrolysis can be categorized as fast (~1,000 °C s^{-1}) or slow (1-20 °C s^{-1}) depending on the temperature ramping rate. Fast pyrolysis is used to produce gaseous and liquid products, while the aim of slow pyrolysis is to produce solid biochar [12,13]. In addition, the residual chars from the fast pyrolysis are physiochemically different than the biochars from the slow pyrolysis. High heating rate affects the surface morphology in terms of loss of cell structure and natural porosity of biochar, while longer residence time results in an enhanced formation of micro- and macropores, and improved specific surface area [14-16].

As the pyrolysis generates relatively cleaner combustion fuel, the indirect combustion of volatiles generated by the pyrolysis of rice husks with subsequent silica separation is an intriguing alternative because of the potential to minimize PM emissions [17]. However, 40% of lignin-carbon remains in the resulting biochar [18,19]. The production of ethanol from rice husk via scarification and fermentation can be another promising alternative to combustion [9,20]. In addition, the fermentation residue is a lignin-rich substrate containing approximately 60% carbon. The residue collected after the fermentation of rice husk has high combustible organic contents (>80% based on the dry mass) with a relatively high calorific value of 23.1 MJ kg^{-1} [21]. Hence, the development of an efficient method that can help utilize the fermentation residue can be a promising direction to replace energy crops and other lignocellulosic biomass resources.

Considering the paucity of studies on the slow pyrolysis of fermented rice husk (FRH), it is important to understand the effect of pyrolysis temperature on the physiochemical properties of biochar produced from FRH to examine its potential utilization as a feedstock in producing high-energy and high-density solid fuels. In this study, the slow pyrolysis behaviors of raw rice husk (RRH) and FRH were compared using a fixed-bed reactor to produce biochar as an energy-dense fuel. The yields, true densities, compositions, and calorific values of the biochars produced from RRH and FRH were compared. The results presented in this study can provide valuable guidelines to evaluate the potential use of FRH.

EXPERIMENTAL

1. Sample Collection and Preparation

RRH samples were collected from a local field in the district of Sheikhupura, Punjab Province, Pakistan. Some of the dust particles in RRH were removed by manual sorting and, subsequently, the RRH was air dried in accordance with the ASTM-D-4931 standard. FRH samples were collected after simultaneous scarification and fermentation of RRH. The details of this fermentation were provided in a previous report [8]. FRH was filtered and rinsed until the solution reached neutrality. Subsequently, the washed FRH was air-dried and kept in airtight bags for future processing. Using a biomass crusher, we crushed all the collected samples to a mesh size of 2 mm for the pyrolysis test and up to 60 mesh for the pre-pyrolysis analyses. The samples were stored in airtight bags.

2. Pre-pyrolysis Analyses

Both the RRH and FRH samples were subjected to different preliminary analyses in accordance with respective ASTM standards. Proximate (i.e., volatile matter (VM), ash, and fixed carbon (FC)) and ultimate analyses were conducted in accordance with ASTM-E-872, ASTM-E-1755, ASTM-D-3172, and ASTM-D-5291, respectively. A Fourier transform infrared (FTIR) analyses was conducted to examine the chemical functional groups using a Perkin Elmer Spectrum FTIR spectrometer with a resolution of 4 cm^{-1} in the range of 4,000-400 cm^{-1}. The true densities of the FRH and RRH samples were measured using a helium pycnometer technique in accordance with DIN-66137-215. Chemical compositional analyses were conducted in accordance with the Tappi standards as described below.

2-1. Estimation of Extractive Content

One gram of the dried biomass sample was dissolved in 60 mL of acetone for 2 h in a round-bottom flask at a temperature of 90 °C. After the dissolution of the extractives, the sample was dried at 105 °C until a constant weight was reached. The amount of extractives in the biomass samples was calculated using the difference between the weight of the biomass before and after the extraction.

$$\text{Extractive content (\%)} = \frac{\text{weight of biomass prior to extraction} - \text{weight of biomass after extraction}}{\text{weight of biomass prior to extraction}} \times 100 \quad (1)$$

2-2. Estimation of Hemicellulose Content

One gram of the extractive-free biomass sample was introduced into 10 mL of 0.5 mol L^{-1} NaOH solution, and the entire solution was maintained at 80 °C for 3.5 h. The hemicellulose-leached biomass was rinsed until the solution became neutral and then dried at 80 °C until a constant weight was reached. The difference in the weights before and after the NaOH treatment was referred to as the hemicellulose content.

$$\text{Hemicellulose content (\%)} = \frac{\text{weight of biomass prior to NaOH treatment} - \text{weight of biomass after NaOH treatment}}{\text{weight of biomass prior to NaOH treatment}} \times 100 \quad (2)$$

2-3. Estimation of Lignin Content

An aliquot (30 mL) of concentrated H_2SO_4 solution was added in an extractive-free dried biomass. The biomass sample in the aqueous concentrated H_2SO_4 solution was stored for 24 h and then boiled for 1 h at 105 °C. After filtration, the residue collected on a filter paper was titrated with 10% $BaCl_2$ solution until the sulfate ions in the filtrate disappeared. The residue was then dried in a heating oven at 105 °C until a constant weight was reached. The difference in the weight before and after the concentrated H_2SO_4 treatment was referred to as the lignin content.

$$\text{Lignin content (\%)} = \frac{\text{weight of biomass prior to } H_2SO_4 \text{ treatment} - \text{weight of biomass after } H_2SO_4 \text{ treatment}}{\text{weight of biomass prior to } H_2SO_4 \text{ treatment}} \times 100 \quad (3)$$

2-4. Estimation of Cellulose Content

The cellulose content was estimated using Eq. (4):

$$\text{Cellulose (\%)} = 100 - (\text{extractives} + \text{hemicellulose} + \text{lignin}) \quad (4)$$

3. Pyrolysis

The pre-weighed quantities of the air-dried RRH and FRH samples were placed in a tube furnace at varying temperatures in the range of 200-600 °C for 1 h at a heating rate of 50 °C min^{-1} under an N_2 flow condition at a rate of 1,500 mL min^{-1}. After reaching experimentally desired temperatures and residence times, the sample was removed from the furnace and desiccated. The weight of the pyrolyzed sample was noted to calculate the weight loss [22].

$$\text{Mass yield (\%)} = \frac{\text{weight of biochar after pyrolysis}}{\text{weight of biomass prior to pyrolysis}} \times 100 \quad (5)$$

$$\text{Mass loss (\%)} = 100 - \text{Mass yield} \quad (6)$$

4. Post-pyrolysis Analyses

All the biochar samples produced by the slow pyrolysis were analyzed as described above. The GCV of the biomass and biochar samples was measured according to ASTM-D5865 using the 1341 bomb calorimeter (Parr, USA). The standard pellet of sample (1 g) was put into the crucible and the bomb assembly was pressurized with oxygen at 2.5 MPa. The bucket of the bomb calorimeter was filled with 2 L of DI water and the bomb was placed into the bucket. Then the whole bucket was put into the jacket of the calorimeter. Fuse wire connections were inserted into their respective holes and the lid of calorimeter was closed with a thermometer inserted to measure the increase in temperature. Stirring was allowed for 5 min prior to starting the combustion reaction. Both the initial temperature of the water (when the experiment was started) and final temperature (when the rise in temperature was stopped) were noted. The GCV was determined as Eq. (7).

$$\text{GCV} = \frac{(M_1 + W) \times C_p \text{ of Water} \times \Delta T}{M_2} \quad (7)$$

where M_2 and W represent mass of biomass (1 g) and of water (2,000 g), respectively, M_1 is water equivalent of calorimeter (357.98 g), C_p is heat capacity of water (1 cal g^{-1}), and ΔT is the difference between the final and initial temperatures.

RESULTS AND DISCUSSION

1. Pre-pyrolysis Characterization

As listed in Table 1, the compositions of the RRH and FRH samples are different. The FRH sample exhibited significantly lower ash content (2.4%) and higher VMs+fixed-carbon content (97.6%) than the RRH sample (61.7% and 12.9%, respectively). In addition, the carbon content of FRH was higher than that of RRH, while the oxygen content of FRH was lower than that of RRH. As a result, the GCV of FRH was significantly greater (19.9 MJ kg^{-1}) than that of RRH (13.2 MJ kg^{-1}) [23,24]. After the fermentation of RRH, the residual, non-fermentable lignin remained in the FRH and increased the total carbon content. The decrease in the mineral content of FRH could be due to its utilization by microbial organisms that were used during the fermentation process [25].

During the fermentation of RRH, cellulose and hemicellulose fractions were consumed whereas lignin remained almost intact because of its high resistance to the biological attack (Table 2); it is much more difficult to decompose lignin compared to cellulose because of its strong 3D aromatic polymer network with a high molecular weight. Thus, the true density of FRH was higher than that of RRH [26].

Table 2. Compositional analyses of RRH and FRH

Sample	Extractives (%)	Cellulose (%)	Hemicellulose (%)	Lignin (%)
RRH	11.0	32.7	15.2	23.6
FRH	17.4	18.24	3.9	58.0

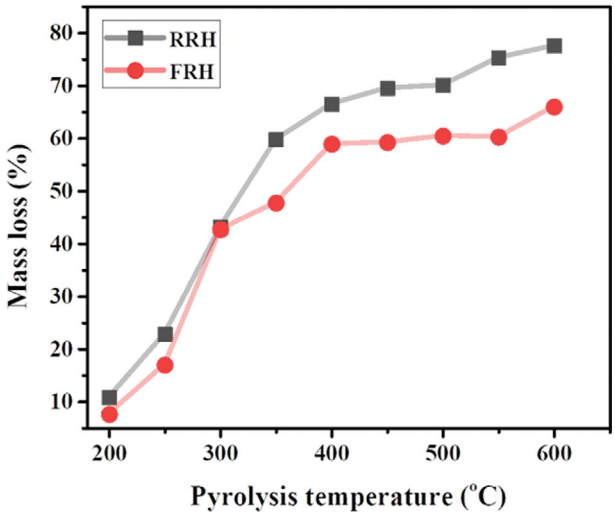

Fig. 1. Mass loss during the production of biochars from RRH and FRH.

2. Biochar Yield

Fig. 1 shows the thermal degradation behavior during pyrolysis. When the pyrolysis temperature reached 200 °C, the mass loss was merely 10.8% for RRH and 7.6% for FRH. Therefore, it was more difficult to degrade the VMs of FRH compared to those of

Table 1. Ultimate and proximate analyses of RRH and FRH

Sample	Ultimate analyses					Proximate analyses[b]			True density (g cm^{-3})	GCV (MJ kg^{-1})
	C (%)	H (%)	N (%)	S (%)	O[a] (%)	VMs (%)	Ash (%)	FC (%)		
RRH	39.9	5.4	1.2	0.1	53.4	61.7	17.6	12.9	1.26	13.2
FRH	43.6	5.5	1.0	0.1	50.1	81.1	2.4	16.5	1.39	19.9

[a]Reported by difference

[b]As-received base for raw and dried base for fermentation

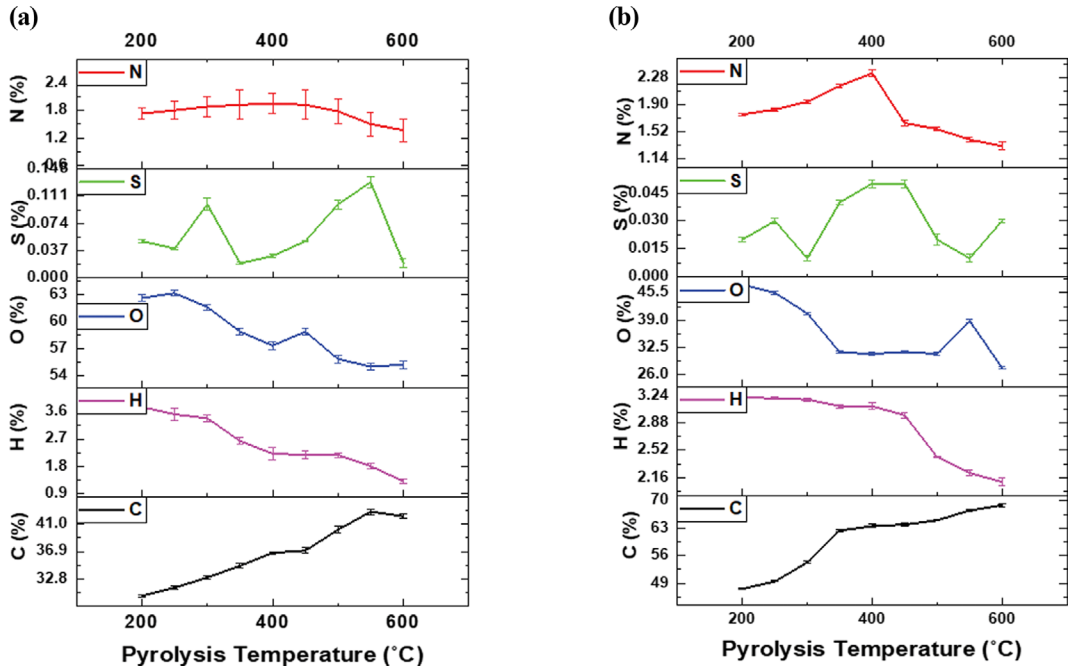

Fig. 2. Ultimate analyses of biochars produced from (a) RRH and (b) FRH.

RRH in the low-temperature regime. When the temperature was raised to 600 °C, the mass losses of RRH and FRH significantly increased to 77.6% and 66.0%, respectively; a low biochar yield in the high-temperature regime resulted from the emission of a significant number of volatiles [27-29]. At the end of 600 °C, the yield of biochar produced from FHR was higher than that produced from RRH, which can be attributed to the facilitated degradation of cellulose and hemicellulose fractions in RRH at high temperatures [30]. Thus, the FRH sample had lower hemicellulose and cellulose content and higher lignin content than the RRH sample, resulting in a lower mass loss at 600 °C. Thus, the biochar yield was directly proportional to the lignin content in the feedstock [18].

3. Ultimate Analyses

When the pyrolysis temperature was increased from 200 to 600 °C, the carbon content in the biochar produced from RRH increased from 30.3% to 42.1%, while the hydrogen and oxygen contents decreased from 3.8% to 1.3% and 62.6% to 55.2%, respectively, which can be attributed to the facilitated evaporation of oxygen-rich VMs and aromatization (Fig. 2(a)). The elimination of -OH, $-CH_3$, $-CH_2$, and -C=O groups during the pyrolysis promoted the aromatization and improved the calorific value [31,32]. The nitrogen content in RRH and FRH reached maximum near 400 °C (i.e., 1.95% and 2.34%), while further increase in the temperature decreased these values to 1.37% and 1.32%, respectively. The increase in the nitrogen content observed when increasing the temperature to ~450 °C can be attributed to the incorporation of N into aromatic structures in the initial pyrolysis stage, which is resistant at low-to-medium temperatures, while the nitrogenated species decomposed at high temperatures [33]. The sulfur content remained low in all the biochars obtained from FRH and RRH (i.e., in the range of 0.01% to 0.13%). Similar trends in the carbon, hydrogen, oxygen, nitrogen, and sulfur content have been observed in a previous work [34]. As shown in Fig. 2(b), the effect of pyrolysis temperatures on the elemental content of the biochar produced from FRH exhibits similar trends to that produced from RRH.

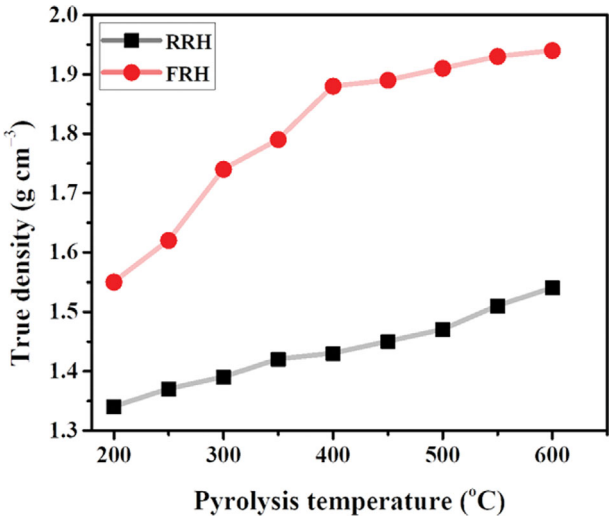

Fig. 3. True densities of the biochars produced from RRH and FRH.

4. True Density

As shown in Fig. 3, the true densities of the biochars produced from RRH and FRH steadily increased with increasing pyrolysis temperature; this indicates the conversion of low-density and disordered carbon to higher-density and turbostratic carbons during slow pyrolysis [35]. The highest values of the true density of RRH- and FRH-derived biochars, 1.54 and 1.94 g cm^{-3}, respectively, were achieved at 600 °C. At the high temperature, the activated pyrolysis of the biomass components resulted in shrinkage of the constituent fragments and increased the number of aromatic carbon clusters [35]. The

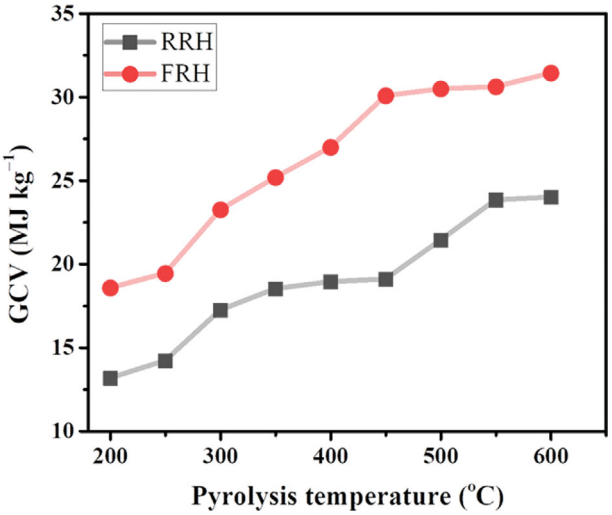

Fig. 4. Gross calorific values of biochars produced from RRH and FRH.

pyrolysis of lignin-rich FRH resulted in consistently denser biochar because the aromatization was facilitated to a greater extent [26].

5. Gross Calorific Values

Fig. 4 shows the GCVs of the biochars produced from RRH and FRH. With the increase in the pyrolysis temperature, the GCVs of both the RRH- and FRH-derived biochars increased. The consistently higher GCVs of the FRH-derived biochars than those of the RRH-derived biochars that were produced at varying temperatures could be due to the higher lignin and extractive content. Both the lignin and extractives contain higher carbon content than those of the other biomass constituents, and thus, the pyrolysis of lignin- and extractive-rich feedstock yielded biochar with a higher GCV. The GCVs of the RRH- and FRH-derived biochars obtained in this study are equivalent to those of high-grade lignite or subbituminous coals, making these biochars highly promising feedstock for use in co-firing applications [36,37].

6. Compositional Analyses

Fig. 5(a) shows the change in the composition and yield of the RRH-derived biochar at varying pyrolysis temperatures. As the temperature was increased from 200 to 600 °C, the cellulose and hemicellulose content decreased rapidly from 29.8% to 4.2% and from 14.6% to 1.2%, respectively [38]. Contrarily, the lignin content increased steadily from 24.5% to 48.6% with increasing temperatures from 200 to 600 °C; this indicates that the residual amount of biochar primarily comprises thermally transformed lignin because of its highly recalcitrant nature [33,36]. The extractive content in the RRH-derived biochars increased from 12.9% to 24.9% with increasing pyrolysis temperature from 200 to 600 °C. Thus, the GCVs of the biomass can be positively correlated with aromatic-enriched lignin content [39]. In addition, extractives, which typically comprise high-carbon-containing phenols, resins, waxes, and long-chain alcohols, can contribute to increasing the GCV of biochar [36,40].

As shown in Fig. 5(b), the lignin content in the FRH-derived biochars increase significantly from 56.9% to 68.0% with increasing temperature from 200 to 600 °C; this is because lignin is the major biomass constituent present in the FRH. Therefore, the FRH-derived biochar produced at 600 °C exhibited significantly higher GCV than the other biochars (Fig. 4) [33]. The mass yields of FRH-derived biochars were consistently larger than those of the RRH-derived biochars. The higher mass yield and higher calorific values of the FRH-derived biochars make them to have higher energy contents as compared to those of the RRH-derived biochars. For example, the total energy content of FRH-derived biochar produced at 600 °C was approximately 36% higher than that of the RRH-derived biochar produced at the same temperature. The minimal condensation of aliphatic compounds and the gradual but higher losses of CH_4, H_2, CO_2, and CO with increasing pyrolysis temperature resulted in cellulose- and hemicellulose-deficient but extractive- and lignin-enriched biochar [39]. Cellulose and hemicellulose have relatively weak chemical bonds, which are prone to thermal decomposition in the low-temperature regime [41]. Thus, the content of residual cellulose- and hemicellulose-derived products was very low (<3.5%) at the highest pyrolysis temperature tested in this study. Contrarily, the aromatic and phenolic groups present in lignin, along with the covalently bonded carbon network, hinder its decomposition in the low-temperature regime [42]. Lignin starts to decom-

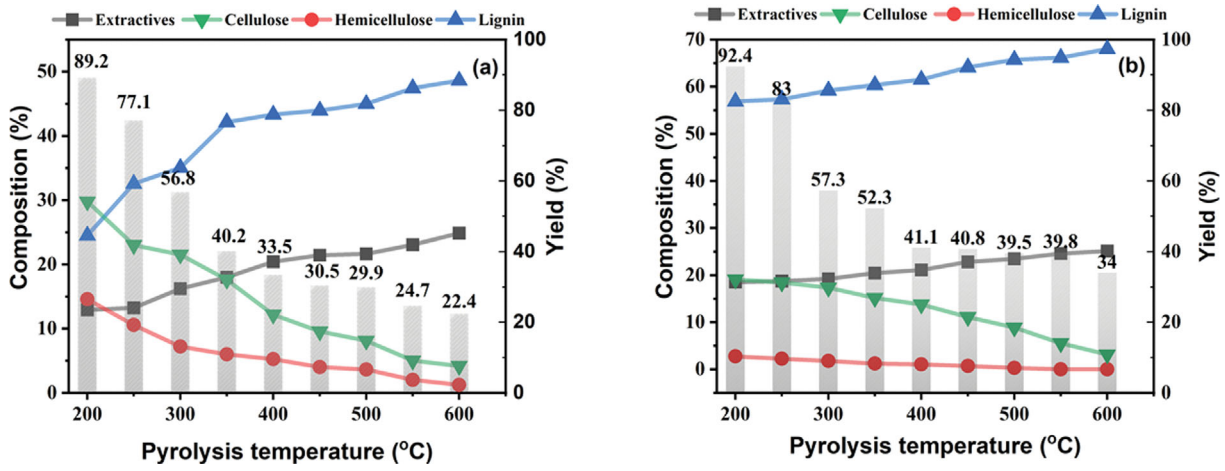

Fig. 5. Compositional analyses and yields (expressed in bars) of (a) RRH- and (b) FRH-derived biochars.

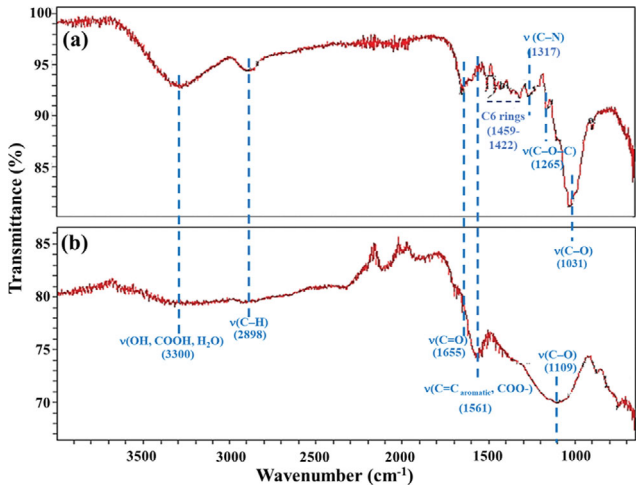

Fig. 6. FTIR spectra of (a) FRH- and (b) FRH-derived biochars produced at a temperature of 600 °C.

pose near 400 °C and covers a wide range of temperatures [43]. Thus, high-lignin-containing biomass is ideal feedstock for the production of high-yield and high-calorific-value biochar [13].

7. Functional Groups Analyses

Fig. 6 shows the FTIR spectra of the FRH and FRH-derived biochars produced at 600 °C. The broad bands at 3,300 and 2,898 cm^{-1} in FRH correspond to the stretching vibration of -OH groups and alkyl C-H, respectively. After pyrolysis, the intensity of the bands associated with -OH and C-H groups decreased significantly. The bands at 1,655 and 1,561 cm^{-1} correspond to the stretching vibrations of C=O and C=C groups, respectively, in the lignin-enriched FRH [44]. The sharp peaks in the range of 1,459-1,422 cm^{-1} in the FRH sample indicate the presence of C6 rings. The small peak at 1,265 cm^{-1} in the FRH sample can be assigned to C-O-C groups, aryl ethers, and phenolic groups accompanied by lignin, which was not observed in the biochar [13]. The intense peak at 1,031 cm^{-1} can be attributed to the C-O group present in FRH [45]. After the pyrolysis, the intensity of the peaks associated with C=O, C-O-C, and C-O decreased, while the peak at 1,561 cm^{-1}, which correspond to the C=C vibration of the aromatic ring, became prominent. Thus, most of the oxygenated chemical functionalities of FRH disappeared after the slow pyrolysis. Nevertheless, some new and well-defined aromatic peaks originated, such as at 2,350, 1,950, 1,561, and 751 cm^{-1}. This may imply that the FRH-derived biochar has high thermal stability and an aromatic structure [46].

CONCLUSIONS

The effect of pyrolysis temperature on the yield and physiochemical properties of biochars produced via slow pyrolysis of RRH and FRH was examined. The FRH-derived biochar exhibited consistently higher carbon content, higher true density, and higher GCVs as compared to those of the RRH-derived biochar. At the high pyrolysis temperature of 600 °C, the FRH-derived biochar had a carbon content of 68.9%, a true density of 1.94 g cm^{-3}, and a GCV of 31.6 MJ kg^{-1}; which indicates that it can be potential replacement of medium-ranked coal. Higher content of lignin-derived (68.0%) and extractive-derived (25.1%) species in the FRH-derived biochar produced at 600 °C is an evidence of enriching with poly-condensed aromatic compounds. This study concludes that fermentation as pre-pyrolysis technique improves the physiochemical properties of the resulting biochar and expands its utilization as an alternative to sub-bituminous rank coal in addition to the applications such as a precursor for producing activated carbons, an adsorbent in separation process, a soil conditioner or a reducing agent in metallurgical applications.

ACKNOWLEDGEMENTS

The authors would like to thank the University of the Punjab, Lahore, Pakistan for financial and technical assistance for this study. Additional support provided by the Korea Institute of Energy Technology Evaluation and Planning (KETEP) by way of granting financial aid from the Ministry of Trade, Industry & Energy (MOTIE), Republic of Korea (No. 2021010000001B) is also appreciated.

REFERENCES

1. Z. Anwar, M. Gulfraz and M. Irshad, *J. Radiat. Res. Appl. Sci.*, **7**, 163 (2014).
2. C. H. Ko, S. H. Park, J.-K. Jeon, D. J. Suh, K.-E. Jeong and Y.-K. Park, *Korean J. Chem. Eng.*, **29**, 1657 (2012).
3. Y. H. Oh, I. Y. Eom, J. C. Joo, J. H. Yu, B. K. Song, S. H. Lee, S. H. Hong and S. J. Park, *Korean J. Chem. Eng.*, **32**, 1945 (2015).
4. L. J. Jönsson and C. Martín, *Bioresour. Technol.*, **199**, 103 (2016).
5. F. R. Vieira, C. M. Romero Luna, G. L. A. F. Arce and I. Ávila, *Biomass Bioenergy*, **132**, 105412 (2020).
6. E. Menya, P. W. Olupot, H. Storz, M. Lubwama, Y. Kiros and M. J. John, *Biomass Convers. Biorefin.*, **10**, 57 (2020).
7. S. Khan, A. Nisar, B. Wu, Q.-L. Zhu, Y.-W. Wang, G.-Q. Hu and M.-x. He, *Sci. Total Environ.*, **814**, 152872 (2022).
8. H. Sana, S. Kanwal, J. Akhtar, R. Haider, S. Nawaz, N. Sheikh and S. Munir, *Energy Sources Part A-Recovery Util. Environ. Eff.*, **39**, 465 (2017).
9. A. Abbas and S. Ansumali, *Bioenergy Res.*, **3**, 328 (2010).
10. L. Dunnigan, P. J. Ashman, X. Zhang and C. W. Kwong, *J. Clean. Prod.*, **172**, 1639 (2018).
11. V. S. Sikarwar, M. Zhao, P. S. Fennell, N. Shah and E. J. Anthony, *Prog. Energy Combust. Sci.*, **61**, 189 (2017).
12. C. E. Brewer, K. Schmidt-Rohr, J. A. Satrio and R. C. Brown, *Environ. Prog. Sustain. Energy: An Official Publication Am. Inst. Chem. Eng.*, **28**, 386 (2009).
13. A. Tomczyk, Z. Sokołowska and P. Boguta, *Rev. Environ. Sci. Biotechnol.*, **19**, 191 (2020).
14. Z. Z. Chowdhury, M. Z. Karim, M. A. Ashraf and K. Khalid, *BioResources*, **11**, 3356 (2016).
15. L. Wang, Y. S. Ok, D. C. Tsang, D. S. Alessi, J. Rinklebe, H. Wang, O. Mašek, R. Hou, D. O'Connor and D. Hou, *Soil Use Manage.*, **36**, 358 (2020).
16. G. Newalkar, K. Iisa, A. D. D'Amico, C. Sievers and P. Agrawal, *Energy Fuels*, **28**, 5144 (2014).
17. Z. Chowdhury Zaira, P. Kaushik, A. Y. Wageeh, S. Suresh, S. Syed

Tawab, A. Ganiyu Abimbola, M. Emy, R. Rahman Faijur and J. Rafie Bin, *Pyrolysis: A sustainable way to generate energy from waste*, IntechOpen Publisher, Rijeka (2017).
18. H.-B. Kim, J.-G. Kim, T. Kim, D. S. Alessi and K. Baek, *Chem. Eng. J.*, **393**, 124687 (2020).
19. A. Demirbaş, *Energy Convers. Manage.*, **42**, 1357 (2001).
20. G. Wu, P. Qu, E. Sun, Z. Chang, Y. Xu and H. Huang, *Bioresources*, **10**, 227 (2015).
21. W. Su, H. Ma, Q. Wang, J. Li and J. Ma, *J. Anal. Appl. Pyrolysis*, **99**, 79 (2013).
22. J. Poudel and S. C. Oh, *Energies*, **7**, 5586 (2014).
23. A. Demirbas, *Energy Sources Part A-Recovery Util. Environ. Eff.*, **29**, 329 (2007).
24. A. Dawei, W. Zhimin, Z. Shuting and Y. Hongxing, *Int. J. Energy Res.*, **30**, 349 (2006).
25. H. Soedjatmiko, R. Chrisnasari and P. H. Hardjo, *IOP Conf. Ser.: Earth Environ. Sci.*, **293**, 012020 (2019).
26. M. Brebu and C. Vasile, *Cellul. Chem. Technol.*, **44**, 353 (2010).
27. S. Kern, M. Halwachs, G. Kampichler, C. Pfeifer, T. Pröll and H. Hofbauer, *J. Anal. Appl. Pyrolysis*, **97**, 1 (2012).
28. X. Cao and W. Harris, *Bioresour. Technol.*, **101**, 5222 (2010).
29. N. Muradov, B. Fidalgo, A. C. Gujar, N. Garceau and A. T-Raissi, *Biomass Bioenergy*, **42**, 123 (2012).
30. A. Demirbas, *J. Anal. Appl. Pyrolysis*, **72**, 243 (2004).
31. X. He, Z. Liu, W. Niu, L. Yang, T. Zhou, D. Qin, Z. Niu and Q. Yuan, *Energy*, **143**, 746 (2018).
32. M. Phanphanich and S. Mani, *Bioresour. Technol.*, **102**, 1246 (2011).
33. M. I. Al-Wabel, A. Al-Omran, A. H. El-Naggar, M. Nadeem and A. R. A. Usman, *Bioresour. Technol.*, **131**, 374 (2013).
34. X. He, Z. Liu, W. Niu, L. Yang, T. Zhou, D. Qin, Z. Niu and Q. Yuan, *Energy*, **143**, 746 (2018).
35. W.-T. Tsai, S.-C. Liu and C.-H. Hsieh, *J. Anal. Appl. Pyrolysis*, **93**, 63 (2012).
36. A. Demirbas, *Energy Explor. Exploit.*, **20**, 105 (2002).
37. S. Liang, Y. Han, L. Wei and A. G. McDonald, *Biomass Convers. Biorefin.*, **5**, 237 (2015).
38. A. Gani and I. Naruse, *Renew. Energy*, **32**, 649 (2007).
39. R. H. White, *Wood Fiber Sci.*, **19**, 446 (2007).
40. T. Bridgeman, J. Jones, I. Shield and P. Williams, *Fuel*, **87**, 844 (2008).
41. P. Kaparaju, M. Serrano, A. B. Thomsen, P. Kongjan and I. Angelidaki, *Bioresour. Technol.*, **100**, 2562 (2009).
42. P. Sannigrahi and A. J. Ragauskas, *J. Biobased Mater. Bioenergy*, **5**, 514 (2011).
43. H. Kawamoto, *J. Wood Sci.*, **63**, 117 (2017).
44. S. Suman and S. Gautam, *Energy Sources Part A-Recovery Util. Environ. Eff.*, **39**, 933 (2017).
45. Z.-H. Lu, L.-T. Li, W.-H. Min, F. Wang and E. Tatsumi, *Int. J. Food Sci. Tech.*, **40**, 985 (2005).
46. X. Zhang, P. Zhang, X. Yuan, Y. Li and L. Han, *Bioresour. Technol.*, **296**, 122318 (2020).